Turkish Journal of Electrical Engineering and Computer Sciences

Volume 29
Number 8 *SI-1*

Article 8

1-1-2021

Classification of P300 based brain computer interface systems using longshort-term memory (LSTM) neural networks with feature fusion

ALİ OSMAN SELVİ

ABDULLAH FERİKOĞLU

DERYA GÜZEL

Turkish Journal of Electrical Engineering & Computer Sciences

http://journals.tubitak.gov.tr/elektrik/

Research Article

Turk J Elec Eng & Comp Sci
(2021) 29: 2694 – 2715

doi:10.3906/elk-2103-9

Classification of P300 based brain computer interface systems using long short-term memory (LSTM) neural networks with feature fusion

Ali Osman SELVİ[1,2,*], **Abdullah FERİKOĞLU**[2], **Derya GÜZEL ERDOĞAN**[3]
[1]Department of Computer Technology, Bilecik Şeyh Edebali University, Vocational School, Bilecik, Turkey
[2]Department of Electrical and Electronics Engineering, Sakarya University of Applied Sciences, Sakarya, Turkey
[3]Department of Physiology, Faculty of Medicine,Sakarya University, Sakarya, Turkey

Received: 02.03.2021 • **Accepted/Published Online:** 09.08.2021 • **Final Version:** 04.10.2021

Abstract: Enabling to obtain brain activation signs, electroencephalography is currently used in many applications as a medical diagnostic method. Brain-computer interface (BCI) applications are developed to facilitate the lives of individuals who have not lost their brain functions yet have lost their motor and communication abilities. In this study, a BCI system is proposed to make classification using Bi-directional long short term memory (Bi-LSTM) neural networks. In the designed system, spectral entropy method including instantaneous frequency change of signal is used as feature fusion. In the study, electroencephalography (EEG) data of 10 participants are collected with Emotiv EPOC+ device using 2x2 visual stimulus matrix prepared on Unity. Each symbol of the 2x2 matrix includes stimulus such as doctor, police, fireman and family. These stimuli are demonstrated to participants with a fixed order. As data collection protocol, 200 ms stimulus time and 300 ms interstimulus interval are used. As the performance success of classification, the average accuracy rates are obtained to be 98.6% for training set and 96.9% for the test set. In addition, in classification of P300 EEG signals, the results obtained via Bi-LSTM are compared with the results obtained using 1 dimensional convolutional neural networks (1DCNN) and support vector machines (SVM) classification methods. Moreover, in the study, information transfer rate (ITR) is provided as 40.39 at an acceptable level.

Key words: Brain computer interface, P300, EEG, Emotiv, Bi-directional long short term memory (Bi-LSTM)

1. Introduction

EEG signals are received by sensors on the scalp. Studies using EEG signals show that EEG data contains a lot of information such as emotion, motor and visual [1]. Recording EEG data is preferred in many studies since it is a non-invasive method. Along with the development of technology, EEG devices are provided with mobile features. With the wireless data transfer facilities, real-time recorded EEG data can be transferred to the computer to process them. Thanks to this advantage, EEG devices have also been used in studies other than medical applications, BCI being one of them [2]. Many BCI systems are designed to be used by people who are paralyzed by chronic neuro-muscular disorders such as amyotrophic lateral sclerosis (ALS), brain stem paralysis or severe spinal cord injury. Recently, systems that enable people to generate commands in the computer environment by using their thinking and focusing abilities are designed. These systems allow people to control various hardware and software by virtue of the interactions, which can be established with the computer environment [2, 3].

*Correspondence: aliosman.selvi@bilecik.edu.tr

In one type of BCI system, the subject is asked to follow a screen where the visual stimulus will be given. The changes expected and observed on EEG signals are called visually evoked potentials [4]. One of these potentials is the signals referred to as P300. P300 signals were first described as positive deflection signals that occurred approximately 300 ms after the stimulus has been shown to the participant in 1965 by Sutton et al. [5].Recently, for individuals who have not lost their brain functions yet have lost their motor and communication abilities, aiding systems are designed using P300 signals to facilitate their lives and to enable them to communicate with their environment [6, 7]. P300-based speller systems are usually formed by displaying flashing characters in different sequences on the computer screen. In Farwell and Donchin's study [8], users were given a visual stimulus consisting of 26 characters on the 6x6 spelling matrix. Participants were asked to focus on the character they wanted to write. As a result of the classification performed step by step using linear discriminant analysis, the characters that individuals focus on were printed on the screen. Gu et al. [9] used a 4x10 spelling matrix with 40 characters in a similar study. In the classification using Bayesian linear discriminant analysis method, a performance of 9.07 character spelling per minute was achieved. However, in these studies, the traditional non-colored P300 spelling matrix was demonstrated as a visual stimulus to the participants. In addition, the oldball paradigm is used in these systems.

Apart from traditional spelling matrices, there are also systems based on 2D or 3D visual symbols. Pérez et al. [10], in his study using the linear discriminant analysis (LDA) classification method, performed a robot arm control with the classification of P300 signals by showing pictures to the participant as visual stimuli, instead of characters. When visual and auditory artifacts were removed, a result was obtained with high accuracy. In another similar study, Iturrate et al. [11] enabled participants to control a wheelchair by giving them visual stimuli using the step-wise LDA (SWLDA) classification method. The performance was achieved with high accuracy. In addition, He et al., in their study, presented four different stimuli in a fixed order and classified them using SVM. They achieved high accuracy results in the classification performed offline on healthy individuals. In the study, it was stated that displaying a small number of stimuli for the participants would provide ease of use in systems designed for patients with severe paralysis and would be advantageous in terms of shortening the classification time [12]. However, traditional methods were used for the classification of visual stimuli in these studies. Moreover, there are methods proposed as hybrid. Wang et al. proposed a hybrid approach on four stimuli in their study. In the study, the participants were given the SSVEP stimulus along with the P300 stimulus [13]. In recent years, with the development of deep learning algorithms, these algorithms have been widely used in BCI systems, as in other areas. Kundu and Arı proposed a deep learning approach for the classification of P300 signals. In their work, instead of creating a single feature matrix, they applied feature fusion by combining two different feature matrices. They specified the feature extraction method based on sparse auto-encoder (SAE) and stacked sparse auto-encoder (SSAE) [14]. The literature doesn't show many studies on the classification of EEG data with LSTM neural networks based on P300 signals. Ditthapron et al. [15], a new comparable study, reported a classification performance success of 83.31% with P300 signals using a LSTM network.

The novelty of the present work against the literature is following: In this study, apart from [8, 9], color stimulus pictures were demonstrated to the participant similar to [10, 11]. In addition, in this study, unlike the traditional P300 paradigm, the stimulus matrix was shown to the participant in a fixed order. In our study, unlike the studies in [10–13], performance results were analyzed using the state-of-the-arts classification algorithms such as 1DCNN and Bi-LSTM networks, in contrast to traditional methods used for classification of P300 signals. Moreover, in this study, unlike the study in [13], performance analysis was achieved without

using the SSVEP component, another feature extraction technique from P300. In this study, instead of the automatic feature extraction method in [14], the feature fusion was applied by combining spectral entropy and instantaneous frequency change in EEG signals containing P300. In our study, EEG data were collected from 10 participants using an Emotiv EPOC+ device. As stimulant, 4 abstract pictures were used, three of them representing medical, security and fire emergencies and one representing the need for calling family members. As data collection protocol, 200 ms stimulus time and 300 ms inter-stimulus interval were used. In the designed system, spectral entropy method including instantaneous frequency change of signal was used for feature extraction. In this study, higher accuracy classification results were succeeded using Bi-LSTM on combining spectral entropy and instantaneous frequency change feature extraction methods. As a result, unlike traditional P300 BCI systems, it was indicated that the proposed method in this study can be used in future studies for bedridden individuals who did not lose their brain functions due to different reasons.

2. Materials and methods

A diagram of the proposed and designed system is given in Figure 1. The visual stimulus shown to the volunteers participating in the test was prepared as animation and shown by a computer. The data collected with the help of EEG device were recorded in sync with animation on the computer. Prior to feature extraction and classification processes, the artifacts occurring due to the hardware structure of the device and the movements of the body were cleared from the EEG data using a IIR Butterworth filter. The features of the filtered data were extracted by the spectral entropy method. The data so readied were classified with the software prepared in MATLAB (MathWorks, Inc., Natick, MA, USA) by using Bi-directional long short term memory (Bi-LSTM) method.

2.1. Participants

A total of 10 healthy adult male volunteers (ages 22 to 50) participated in test procedures in the study. All participants are university graduates and use their right hands. The average age of the volunteers participating in the study was 36.8 years. The participants were informed about the 28.12.2016 dated and 16214662/050,01,04/2 numbered experimental protocol, which was approved by the Ethics Committee of the Sakarya University Faculty of Medicine. All participants informed about the details of the experimental protocol signed a voluntary consent form of which a copy was delivered to them. The basic criteria were determined for the participants in order to obtain EEG data under the same conditions and to minimize the artifacts during the process of recording data.

The following criteria were taken into consideration while including the volunteers in the study:

- being between the ages of 18–65.
- giving consent to participate in the study,
- having no known neurological or psychiatric disorder,
- not having received any pharmacological agent that may affect cognitive functions in the last month,
- not having consumed drinks containing caffeine such as coffee, tea, soda, etc. on the day of the test, not having used chemical like hair styler on the hair and having a clear hair.

2.2. EEG data recording

The Emotiv EPOC+ EEG device used to record the data in the study is shown in Figure 2. The device from Emotiv Company, which is preferred in BCI studies due to its mobile feature, offered the opportunity to record

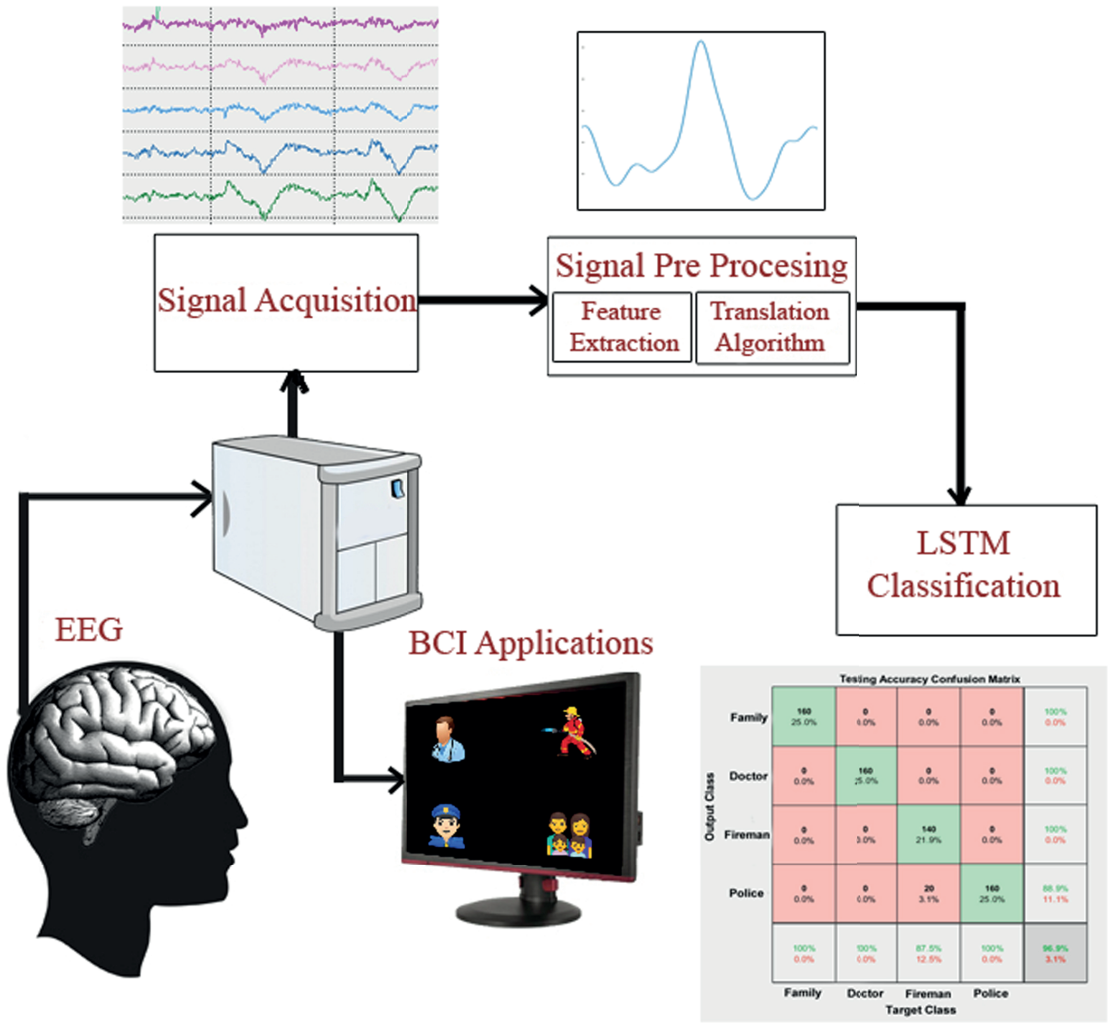

Figure 1. Proposed P300 based BCI system structure.

EEG data in real time [16, 17]. The data obtained from the participants were transferred to and then analysed in the MATLAB (Natick, MA, USA). EEG device can record data with 14 channels. There are sensors on the skull at the points AF3, AF4, F3, F4, FC5, FC6, F7, F8, T7, T8, P7, P8, O1, O2. The system was capable to take 128 or 256 samples a second from each channel. In addition, it provided wireless connection from the EEG device to the computer. The EPOC+ device uses disposable wet salt-based sensors as opposed to gel devices. In addition, this device offers limited contact compared to gel-using EEG devices. Therefore, if the signal attenuation is encountered during the data recording phase, the participant is asked to repeat the test procedure to ensure that the data is of the same quality.[1]

The amplitude range of the recorded EEG data was 1–100 µV (peak to peak) and the frequency range was 0.5–20 Hz. The frequency, phase and amplitude of the EEG signals change continuously because they are not periodic [18–20]. The participants were informed about the experimental procedure, and the study before

[1]EMOTIV (2019). Emotive EPOC+ Device [Online]. Website https://www.emotiv.com/epoc/ [accessed 26 February 2021].

the data acquisition process started. In addition, a sample trial was conducted for each participant before the data acquisition process so that they were adapted to the system. As the P300 EEG data are obtained from the participants, they are aligned with the monitor as shown in Figure 3 and are seated in front of the monitor so that there is a distance between 60 and 80 cm. EEG data were collected using a computer with Intel i7 6700 HQ 64-bit processor, 24 Gb RAM, 22'' monitor and Windows 10 operating system. The EEG recording is performed with EPOC+, sampling frequency is determined as 128.

Figure 2. Emotiv EPOC+ device used in this study.[1]

Figure 3. EEG data acquisition from participants in the study.

2.3. Visual stimuli matrix

In the study, a 2x2 P300 visual stimuli matrix shown in Figure 4 was prepared as desktop software on Unity. The participants are shown a 2x2 P300 matrix created by placing colour pictures on a black background.

In this study, a stimulation method different from traditional P300 spelling matrices is proposed. The spelling matrices in BCI systems are generally systems based on textual writing [3, 8]. In these systems, alphabetic characters are shown to the participant as a stimulus. Especially, giving excessive stimuli in P300 systems applied in bedridden individuals makes it difficult to train the systems and follow the stimulus. Therefore, there is a need to design a P300 system with few stimuli. [12]. In this study, unlike the traditional

P300 paradigm, a fixed order stimulus demonstration method is applied. There are the proposed similar approaches in previous studies [12, 21]. The purpose of this is to respond to the focused stimulus with the help of a single stimulus series, rather than determining which stimulus occurs more in the P300 signal with many stimulus trials. In the P300 visual matrix given in Figure 5, a picture of doctor (P1) representing health emergency, a picture of policeman (P2) representing security emergency, a picture of fireman (P3) representing fire emergency and a family picture (P4) representing a need for seeing a family member prepared with Unity program were shown to 10 different individuals. The pictures remained on the screen for 200 ms in same orders. Inter-stimulus interval was 300 ms. The working procedure of the stimulus matrix was shown to the participants. The progression from P1 to P4 was shown for the time sequence pictures. The progression process from P1 to P4 is repeated as each reminder was considered a stimulus.

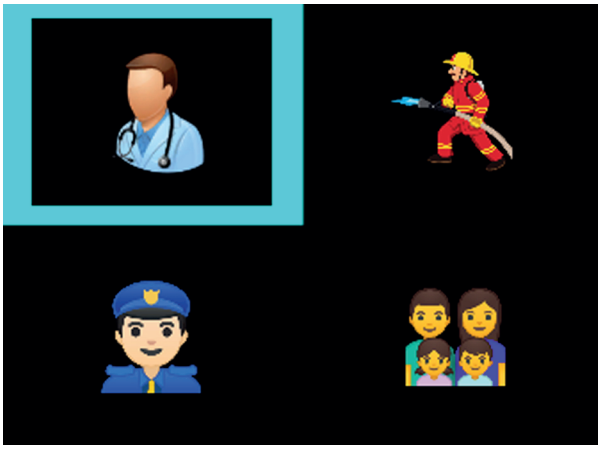

Figure 4. The designed P300 stimulus matrix.

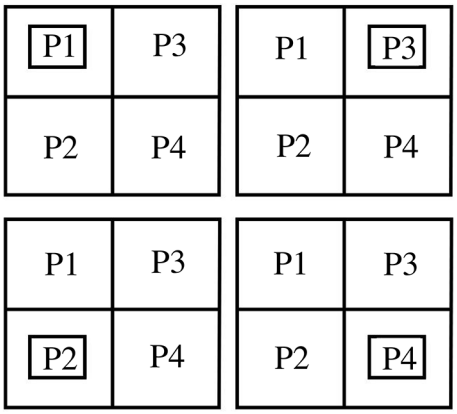

Figure 5. Proposed P300 stimulus matrix. The boxes from P1 through P4 stand for time sequenced pictures.

When the animation is started, the participants are shown a 3 s countdown screen followed by a 5.6 s black blank screen. For 2 s after the black screen, all stimuli are displayed on the screen. Meanwhile, a green border is shown around the symbol for which the participant is required to focus. In the study, if the stimulus focused by the participant appears on the screen, the participant is not asked to perform a task for marking on the data. 600 ms black screen is shown to the participants before the stimuli are displayed one by one since they

could be used as reference data in the data processing phase. Afterwards, the participants are switched to their neutral states. The duration of the stimuli to be displayed to the participant is 200 ms and the inter-stimulus interval (ISI) is 300 ms. This process is repeated 16 times for 1 symbol. The data collection scenario applied to be used in training and testing steps of classification methods can be seen in Figure 6. In this scenario, 16 repetitions were performed for each stimulus while data was collected from the participants. In this way, a P300 EEG signal containing 16 Doctors, 16 Police, 16 Fireman and 16 Family stimuli was created from each participant. This procedure was applied to 10 participants, and EEG signals containing 64 different P300s were obtained for each participant. The total time for data acquisition is 3 min and 5 s for each participant.

When the signal patterns in the graphs in Figure 7 are evaluated, the P300 signals formed after approximately 300 ms for the participant focused on the Doctor in (a), the Police in (b), the Fireman in (c), and Family in (d) stimuli, are seen respectively. As a result, it is seen that the P300 signal is formed separately for 4 stimuli, with the stimulus sequence being in a fixed order. In Table 1, the stimulus class symbols identified for four different stimulus classes are shown as A, D, I and P for the family, doctor, fireman and policeman, respectively.

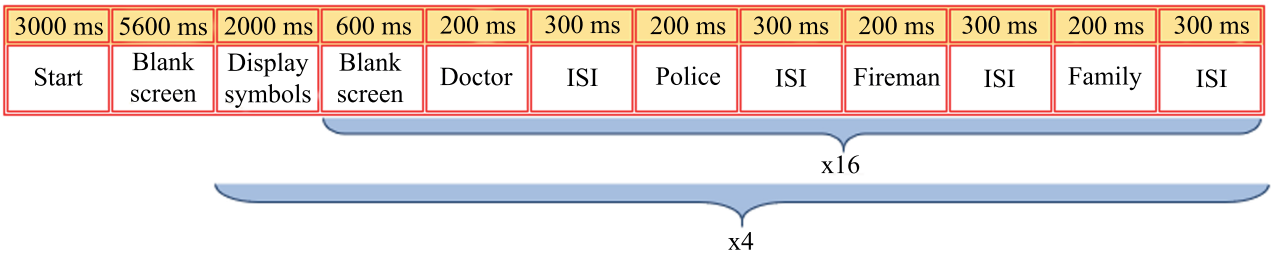

Figure 6. Stimulus period and inter-stimulus interval.

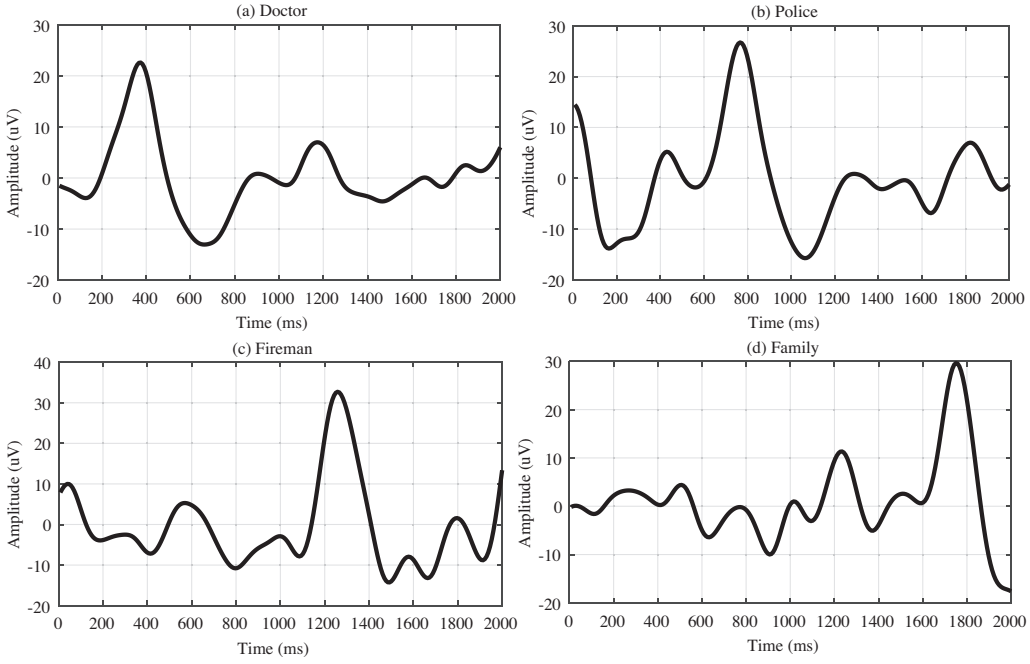

Figure 7. P300 signal patterns formed in fixed order for 4 different symbols.

Table 1. The symbolic expression of visual stimulus classes.

Stimulus type	Matrix symbolic expression
Family	A
Doctor	D
Fireman	I
Policeman	P

An acquired P300 signal pattern is shown in Figure 8 for the doctor's stimulus. While the signal was recorded, all stimuli were shown to the participant in a fixed order. In the P300 signal generated for this stimulus, the stimulus duration and the ISI duration of the stimulus are presented in parts in the time plane. This signal pattern begins with the end of the black screen given before 600 ms stimuli in pre-processing. While the signal was being recorded, the participant was asked to focus on the stimulus of the Doctor. This stimulus remained on the screen for 200 ms from the start of the formation of the EEG data. In this signal, it is seen that the P300 signal is formed after 200 ms, and the response signal is completed when the initiation of the Police stimulus approached approximately 500 ms. If the participant were asked to focus on another stimulus, the Police, the P300 would have formed in the following 300 ms, as the Police stimulus would be issued for 200 ms from the start of the part indicated as Police on the time plane. In summary, the P300 signal is generated in the parts where the stimulus is given in the same time period for each stimulus. In this way, 4 different EEG signal patterns representing 4 stimuli are obtained.

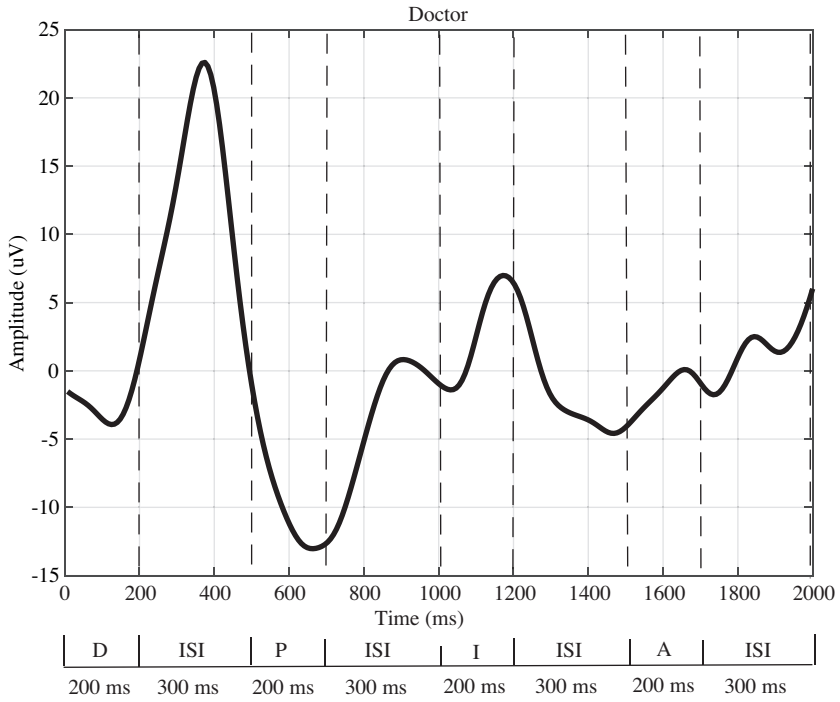

Figure 8. P300 signal pattern for Doctor stimulus.

2.4. Filtering of EEG signals

In this study, due to the convenience of changing the filter time constant for different data group applications, the amplitude based shifting process is corrected by using a filter with infinite impulse response so as not to disorder the original structure of the signal. The code syntax of the filter is given in Algorithm I[2].

Algorithm 1: Matlab syntax for shifting correction.

```
Result: EEGdata
initialization :
Read EEG_D, Row Column Size from Raw EEG Data
Sampling Rate SR = 128
Create EEGdata matrix form of zeros
Create back_eeg matrix as a duplicate matrix EEG_Data
for r1 = 1 to size Row do
    for r = 2 to size Row do
        instructions ;
        Calculate back_eeg(r1) of (back_eeg(r1) * (SR-1) + EEG_D / SR);
        Calculate EEGdata(r1) of EEG_D(r) - back_eeg(r1);
    end
end
```

In order to produce a meaningful signal from the EEG, it has to be examined on the amplitude and frequency components. When the EEG data are implemented into a real application, a plurality of artifacts interferes. Artifact causes the potential between the electrodes to change in some way. Eye movements, coughing, blinking and hand movements during EEG data recording are examples of these potentials [22]. Analog filter designs are used for hardware solutions. Filters designed for the system can be manufactured by the EEG recorder manufacturer and included in the system. Reducing the effects of frequencies other than the desired frequency is usually achieved by discrete fourier transform (DFT), finite impulse response (FIR) and infinite impulse response (IIR) filters [23, 24]. Although IIR filters are linear filters like repetitive FIR filters, they benefit from the last M (number) samples as well as the last P (number) filters. In this way, IIR filters operate with fewer coefficients. Butterworth, Tchebychev or Elliptic filters are often used in EEG signal analysis [25, 26]. The mathematical function of the IIR filter is given in Equation 1. The digital filter function operates in the form of repeated multiplication and addition. Where ak and bk represent filter coefficients, x(n) and y(n) represents the input and output signal sequences, respectively. M and P also indicate the degree of the filter. These two coefficients are used equally since the simple filtering is adequate [27].

$$y(n) = \sum_{k=0}^{N} a_k s(n-k) + \sum_{k=1}^{P} b_k y(n-k) \tag{1}$$

2.5. Feature extraction and feature fusion on EEG signals

EEG signal becomes a complex signal containing many different information. For this reason, the desired signal structure has to be obtained using feature extraction from the EEG signal with different techniques. Therefore, in this study, feature vectors were created by examining the instantaneous frequency changes of the spectral entropy obtained from EEG signal [28]. Attribute vectors for classification algorithms have to be established

[2]EMOTIV (2019). TestBench User Manual [Online]. Website http://physics.hpa.edu/sandbox/users/dao_v/weblog/9320d/attachments/a8987/Te
Manual.pdf [accessed 11 June 2019].

before applying EEG data to the Bi-LSTM network. As the feature extraction method, spectral entropy including the instantaneous frequency change of the signal is calculated to determine the energy changes over time as the feature extraction method for increasing the classification performance [29]. It is aimed to increase the classification performance with the proposed feature fusion system. Feature fusion data consists of two P300 signal features. One of these features is the spectral entropy technique used in spectrum analysis of the signal. Another is the instantaneous frequency changes in the signals. The basic spectral entropy expressions used in feature extraction are given in Equation (2) and Equation (3).

$$SEN = -\sum_{k=1}^{M} (\theta \log_2 \theta) \tag{2}$$

where θ is expanded as,

$$\theta = |z_x[k]|^2 / \sum_{k=i}^{M} |z_x[k]|^2 \tag{3}$$

Here, $z_x[k]$ is the Fourier transform of the analytic similarity matrix z[n] derived from the raw data x(n). M is the length of the $z_x[k]$ signal obtained by Fourier transform [30, 31]. The signal-power spectrum output of 1 participant at 15 Hz frequency resolution via feature fusion is shown in Figure 9 (a).

Instantaneous frequency changes are an important feature used for non-constant signals. P300 signals cause instantaneous changes in signal frequency in addition to changes in amplitude. The basic instantaneous frequency is given in Equation (4) where φ(t) is instantaneous phase[32]. The instantaneous frequency for each type of stimuli is shown Figure 9 (b).

$$f(t) = \frac{1}{2\pi} \frac{d\varphi(t)}{dt} \tag{4}$$

2.6. Long short term memory (LSTM) neural network

Long short-term memory (LSTM) is a type of recurrent neural network (RNN) that can predict the capacity of repetitive sequences by self-feedback. Although each RNN node in the LSTM structure has internal memory capable of generating an irregular array, the disappearance or growth of the gradient problem for RNN is problematic for these networks. To eliminate such problems, an LSTM network was developed by adding 3 gates into the RNN cell. These 3 gates are gi(t) (input gate), fi(t) (forget gate) and qi(t) (output gate). In addition, the input gates control the flow of new information entering the cell. The forget gate decides whether the data are stored in the cell. The output gate is activated when the output is produced. There is a state unit at the base of each gate si(t). gi(t), fi(t), si(t) and qi(t) equations are given in the following Equations (5, 6, 7, 8, 9), respectively.

$$g_i^{(t)} = \sigma\left(b_i^g + \sum_j U_{i,j}^g x_j^{(t)} + \sum_j W_i^g h_j^{(t-1)}\right) \tag{5}$$

$$f_i^{(t)} = \sigma\left(b_i^f + \sum_j U_{i,j}^f x_j^{(t)} + \sum_j W_i^f h_j^{(t-1)}\right) \tag{6}$$

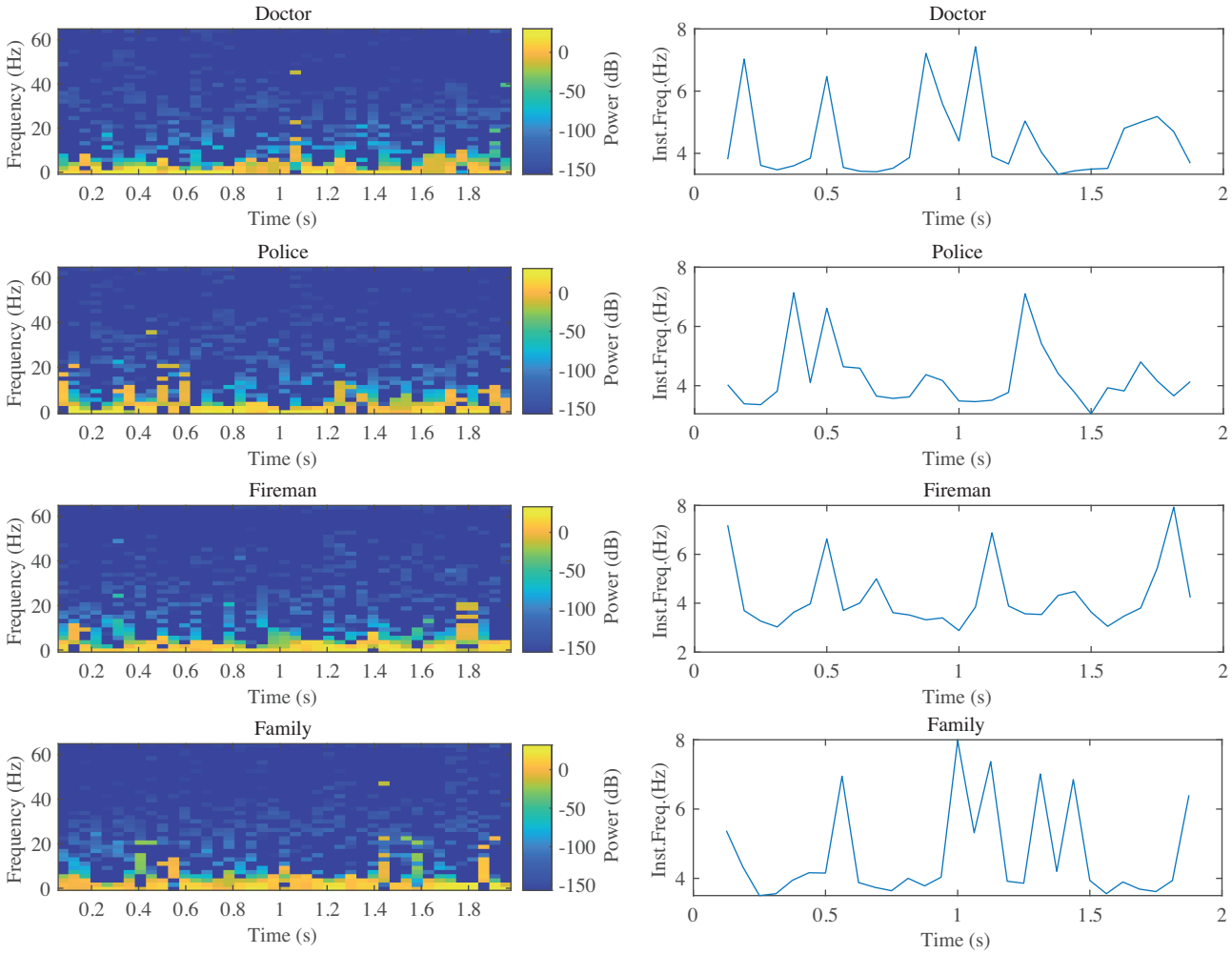

Figure 9. (a) Signal-power spectrum at 15 Hz frequency resolution. (b) Instantaneous frequency for each type of stimuli.

$$s_i^{(t)} = f_i^{(t)} s_i^{(t-1)} + g_i^{(t)} \sigma \left(b_i + \sum_j U_{i,j} x_j^{(t)} + \sum_j W_i h_j^{(t-1)} \right) \tag{7}$$

$$h_i^{(t)} = \tanh \left(s_i^{(t)} \right) q_i^{(t)} \tag{8}$$

$$q_i^{(t)} = \sigma \left(b_i^0 + \sum_j U_{i,j}^0 x_j^{(t)} + \sum_j W_i^0 h_j^{(t-1)} \right) \tag{9}$$

Here U is the weight matrix connecting the inputs in the active latent layer, W is the weight matrix connecting the previous latent layer and the active latent layer. 'b' is bias. 'i' is the subsymbol of U, W, and b shows the filter number. x (t) is the active input vector, and hi(t) is the active latent layer. 'i' denote the connected cell, t is the time step in each cell. σ is a sigmoid function that acts as a gate in the LSTM unit [15].

The Bi-LSTM network proposed in the study is designed as five layers as shown in Figure 10. First, 29 kernel entries of 1x2 size are placed in the first layer in the form of NxMx29 blocks. Then, a 1x2 Bi-LSTM block is added to determine the output of the network. Subsequent layers are suitable for the network. It is interconnected by a fully connected layer placed in the third layer. The Bi-LSTM layer and a softmax layer are used to transfer the most suitable filters to outside of the network. In the last stage, a classification layer provides the appropriate classification of four different stimuli. Thus, EEG signals containing visual stimuli are automatically classified with this established deep Bi-LSTM network [33, 34]. In this study, Bi-LSTM network, a type of LSTM neural networks, was used to classify P300 signals. In the Bi-LSTM network, $\overrightarrow{h(t)}$ in the hidden layer represents the forward model from the first Bi-LSTM unit, while $\overleftarrow{h(t)}$ denotes the backward model from the last Bi-LSTM unit [35] . Besides, in this study, the proposed network was regularized using 20% droput in the Bi-LSTM network. In addition, in the Bi-LSTM network, the "Adam" function was used as an optimizer, and the learning rate was specified as 0.001.

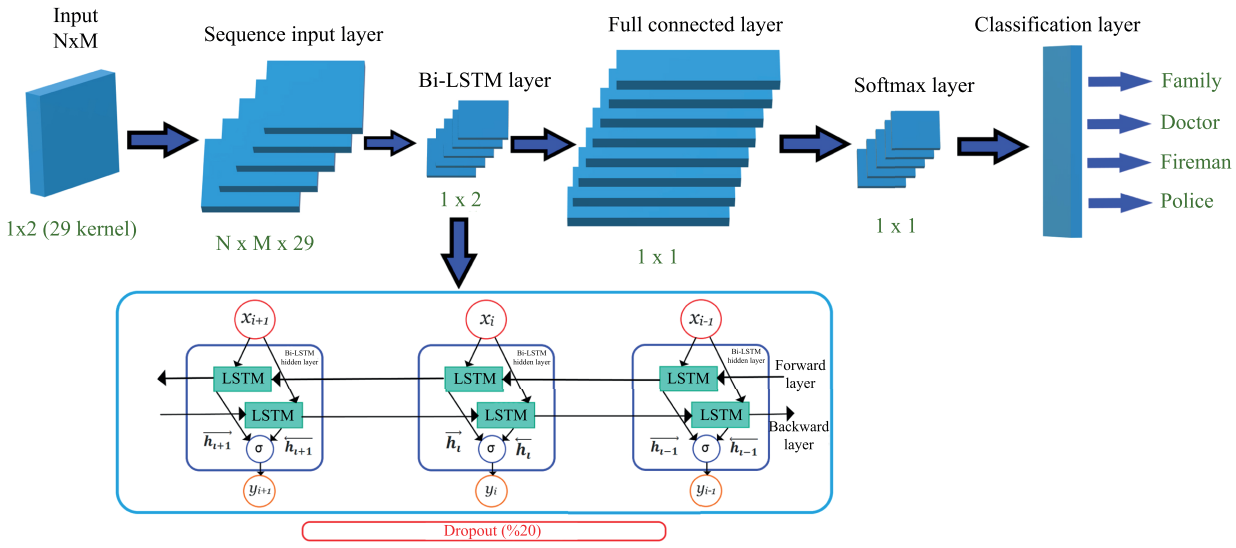

Figure 10. Proposed deep neural network architecture with Bi-LSTM for this study.

3. Results

The noise-free EEG data samples were allocated as 90% for training and 10% testing. Since the total number of data in the dataset is low, data augmentation was performed for both training and test sets, and the total number of data in both sets was increased 10 times. In the experimental setup prepared in the study, each visual stimulus is expressed with a symbolic letter.

When the filtered signals are applied to the Bi-LSTM network without feature extraction, the network completed the training with 25% accuracy. The accuracy gives the rate of classification of the values predicted with the target in the classification process. The loss represents the difference between the predicted and the targeted value. After this training, the Bi-LSTM network, to classify for 4 stimuli, included all symbol groups into a single class. The classification results of the training set obtained without feature extraction are shown

in Figure 11 (a) using the confusion matrix, where the distribution of classification results for 4 classification groups resides. All the input data for the 4 focuses are included in the output layer only in the Doctor class. Although the performance for the Doctor class is 100%, it was not considered an acceptable performance rate because all data are included in a group. For the same reason, the average performance of the confusion matrix is 25% for all focus groups. However, the classification score for the other 3 classes could not be obtained due to the inability to make an evaluation. The results of the test set are given in Figure 11 (b). Figure 11 (b) reveals that, when all focuses are included in the Doctor group, the classification performance is 100% for the Doctor group and 0% for the other classes. The average classification performance is 25%, as in the classification of test set.

Training Accuracy Confusion Matrix

Output Class	A	D	I	P	
A	*0*	*0*	*0*	*0*	
D	*1440*	*1440*	*1440*	*1440*	25% 75%
I	*0*	*0*	*0*	*0*	
P	*0*	*0*	*0*	*0*	
Accurate	0%	100%	0%	0%	25%
Error	100%	0%	100%	100%	75%
	A	D	I	P	
	Target Class				

(a)

Test Accuracy Confusion Matrix

Output Class	A	D	I	P	
A	*0*	*0*	*0*	*0*	
D	*160*	*160*	*160*	*160*	25% 75%
I	*0*	*0*	*0*	*0*	
P	*0*	*0*	*0*	*0*	
Accurate	0%	100%	0%	0%	25%
Error	100%	0%	100%	100%	75%
	A	D	I	P	
	Target Class				

(b)

Figure 11. (a) Bi-LSTM training results without feature fusion. (b) Bi-LSTM testing results without feature fusion.

The obtained data were taken as the average of spectral entropy values by instantaneous frequency analysis, and EEG data are subjected to standardization process with the standard mean and standard deviation of the training data. It is seen in Figure 12 that the accuracy success rate increases from 25% to 98.6% when the feature extracted EEG signals are applied to the Bi-LSTM network. The confusion matrix of Figure 13 (a)for the training set denotes the classification results for 4 focuses. For family and doctor, a 100% performance is achieved in the classification results. It is seen that, in the data group of the Fireman, 80 samples were misclassified as policeman focal points. As a result, the performance rate of the fire department was found as 94.4%. From the confusion matrix, it is also seen that all the samples of policeman data were correctly classified. However, the inclusion of 80 samples from the fireman group sets the performance of the policeman focus at 94.7%. Thus, the average performance rate for all classes is 98.6%. The classification results for the test data in the confusion matrix in Figure 13 (b) denotes that classification success is 100% for Doctor and Family groups for both Bi-LSTM output class and target class. However, for Fireman, Bi-LSTM output class success is 100%, but target class success is 87.5%; for Policeman, Bi-LSTM output class success is 88.9%, but target class success is 100%. These discrepancies for Policeman and Fireman are due to misclassification of some fireman as police. Thus, the average performance rate was found as 96.9% for test samples.

In this study, feature fusion with spectral entropy and instantaneous frequency from EEG signals containing P300 was performed. In addition, in order to verify the performance of the proposed method, P300 signals

generated with four different stimuli were classified by extracting characteristics with Welch's method, which is a traditional method. Welch's method is a periodogram method based on FFT [36]. Frames of different sizes to obtain the power spectrum density of the EEG signals in the frequency plane evaluate the time series signal in sections. In the study, 256 windows are used for each signal segment in the feature extraction process using the welch method. Feature matrices were obtained with 129 features extracted from these windows (256/2+1=129).

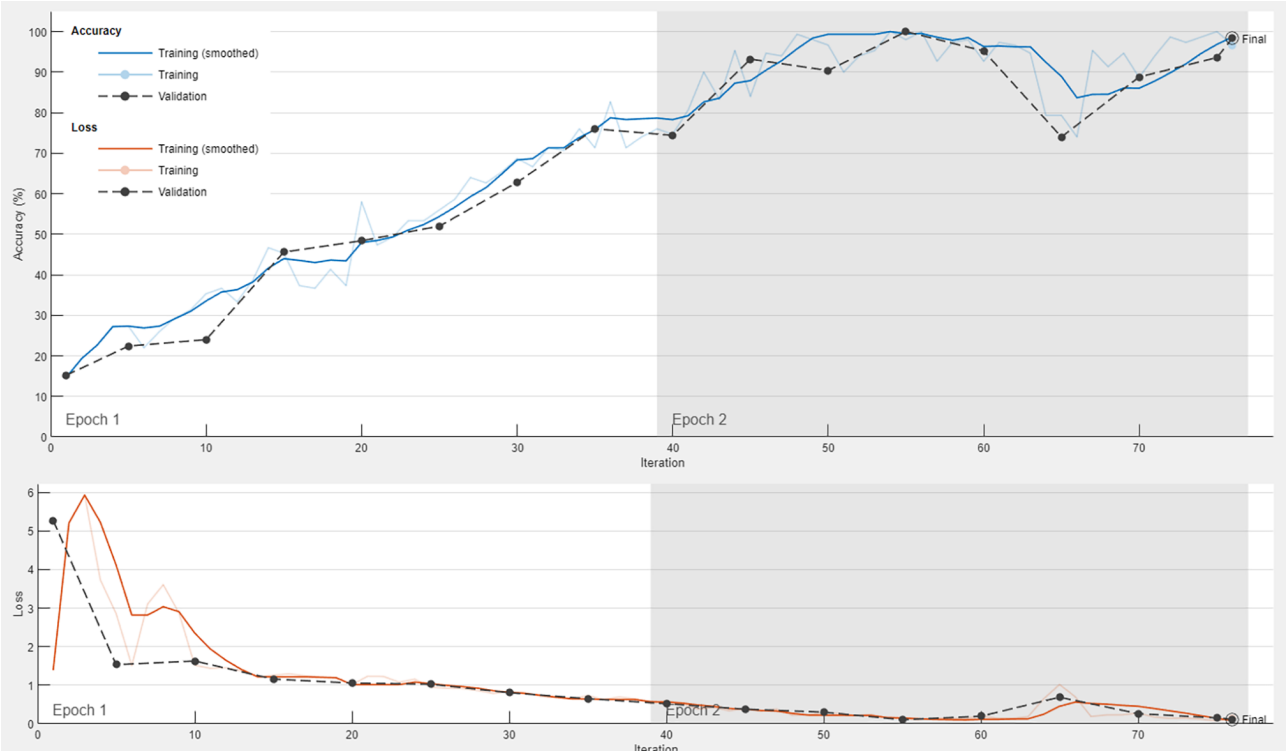

Figure 12. LSTM training performance with feature extraction.

The confusion matrices denoting the classification performance using the features obtained from the Welch method are indicated in Figure 14. When the confusion matrix for training in Figure 14(a) is evaluated, different numbers of false positive classifications are seen for all other symbols except for the A symbol. It is seen that the average training performance was achieved as 92.4%. According to the confusion matrix for the test data in Figure 14(b), it is seen that the average performance is at 90.6%. This classification rate is 6.3% lower than the Bi-LSTM network classification of the features obtained with the feature fusion technique. On the other hand, it is seen that the Bi-LSTM architecture achieves a higher classification performance from the feature data generated by spectral entropy and instantaneous frequency components of the EEG signal compared to the feature data obtained by Welch's method.

In order to evaluate the performance of the proposed Bi-LSTM architecture, the results obtained in this study were compared with the results obtained in support vector machine (SVM), one of the traditional methods, and the 1DCNN architectures, one of the-state-of-the-arts classification methods, in the classification of P300 data. SVMs are one of the pattern recognition methods used in the classification of P300 signals [37]. In this study, an SVM structure providing multiple classification with Gaussian kernel function is used. 1DCNN is one of the deep learning architectures widely used in signal processing applications [38, 39]. Since

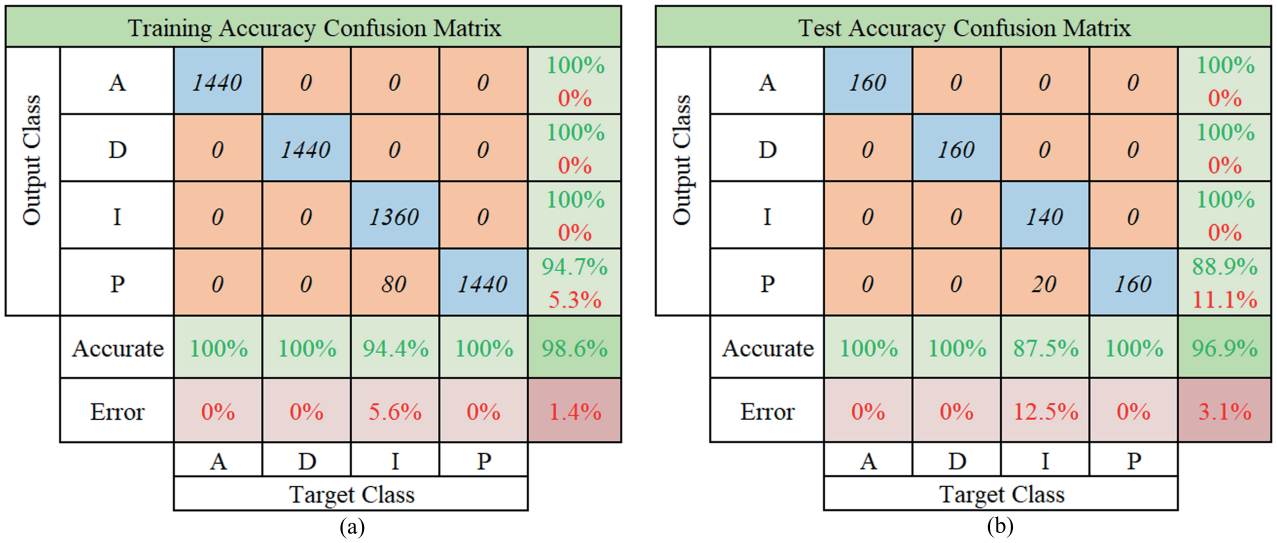

Figure 13. (a) Bi-LSTM training results with feature fusion. (b) Bi-LSTM testing results with feature fusion.

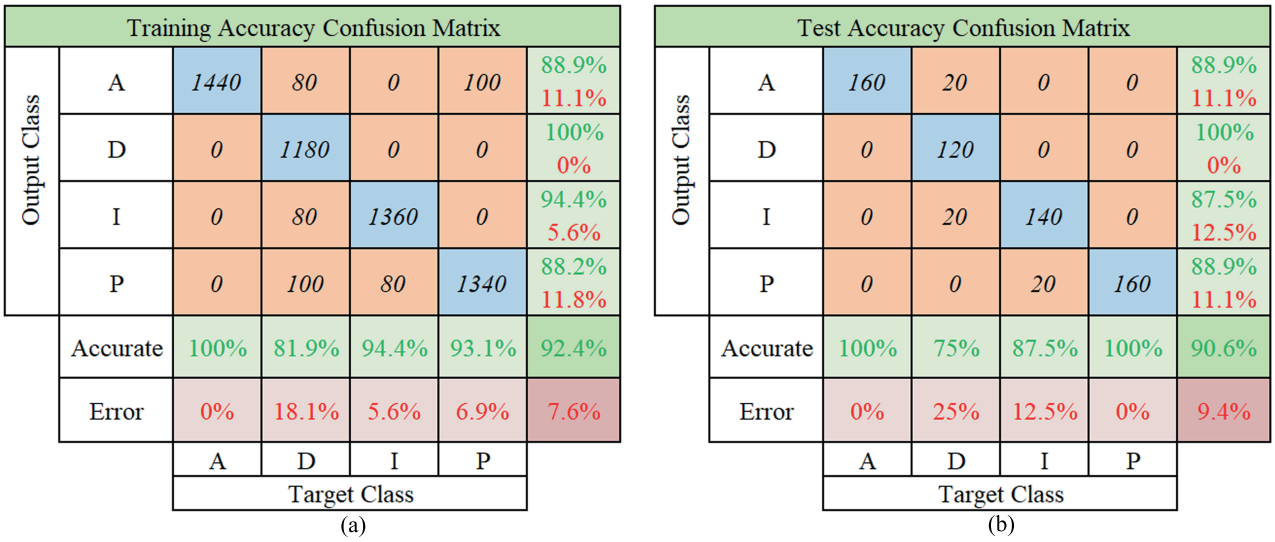

Figure 14. (a) Bi-LSTM training results with Welch feature. (b) Bi-LSTM testing results with Welch feature.

Bi-LSTM neural networks proposed in this study have a deep learning architecture, the results achieved with Bi-LSTM in this study were compared with the results obtained with 1DCNN. Thus, the results of the proposed method were verified. The comparison of the results obtained using the P300-supported BCI system based on the proposed Bi-LSTM architecture and including the feature fusion technique, with SVM and 1DCNN classification methods previously used in similar systems is shown in Figure 15. The confusion matrix given in Figure 15(a) was obtained as a result of the SVM classification on the features obtained by the feature fusion technique. As a result of the classification according to this confusion matrix, the average performance was performed to be 93.8%. From this confusion matrix, it can be seen that in features applied with feature fusion, 20 samples for the A symbol are classified as I symbols, and 20 samples with D symbols are classified

as P symbols. The confusion matrix denoted in Figure 15(b) is obtained as a result of the classification on features extracted by feature fusion technique with 1DCNN network. According to this confusion matrix, an average accuracy of 95.3% was obtained as a result of the classification using feature fusion features. From this confusion matrix, it can be seen that 10 examples for D symbol are classified as P symbols and 20 examples with P symbols are classified as A symbols.

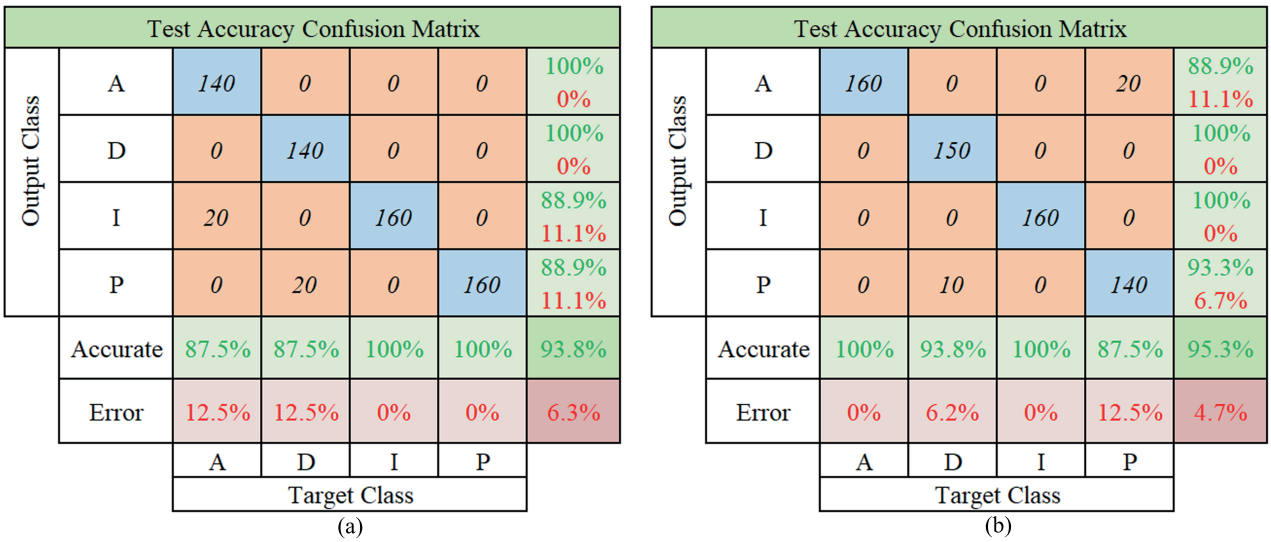

Figure 15. (a) SVM testing results with feature fusion. (b) 1DCNN testing results with feature fusion.

Using the EEG signal data obtained from the proposed P300 system in this study, a feature extraction consisting of the combination of spectral entropy and instantaneous frequency was carried out. To compare the performance of these feature fusion features, the features extracted by the Welch method were used in the proposed Bi-LSTM architecture, 1DCNN and SVM classification methods, respectively. The results obtained are summarized in Table 2.

Table 2. Information transfer rate values according to classification success.

Method	Test accuracy	Test error	ITR
LSTM with feature fusion	96.9%	3.1%	40,4189
LSTM with Welch	90.6%	9.4%	32,3384
SVM with feature fusion	93.8%	6.2%	36,1477
1DCNN with feature fusion	95.3%	4.7%	38,1229

According to the classification results in the test set, the highest performance was achieved using the Bi-LSTM architecture with 96.9%. These results are obtained by the combination of spectral entropy and instantaneous frequency methods. Following Bi-LSTM, the proposed feature fusion method using 1DCNN architecture achieved the highest performance with 95.3%. In the classification studies carried out, it was evaluated that P300 signals with more than one feature achieved higher success in classification. Using the proposed Bi-LSTM architecture, higher performance in the classification of EEG data compared to SVM method indicates that the Bi-LSTM network structure is successful and effective in classification on P300 signals. In

traditional P300 spelling systems, participants are given stimuli in the form of a row-column matrix. In such systems, P300 signals are classified as binary as a result of many repetitions. Apart from these systems, it is seen in previous studies that there are different stimulation techniques from the row-column paradigm for stimulus matrices. In this study, using the advantage of a small number of stimuli in a P300 system with fewer stimuli, all stimuli were demonstrated to the participant in a fixed order. Thus, the recorded EEG data were classified as a whole until the display of the stimuli was completed. The amount of data that the system can transfer per minute is one of the important features of P300 systems. One of the performance criteria of P300 BCI systems is the information transfer rate (ITR). In traditional BCI systems, the stimulus for P300 classification is shown to the participant with many repetitions. The use of such systems causes an increase in the time taken to identify a stimulus as seen from the ITR definition presented in Equation 10, Equation 11 and, thus, a decrease in the ITR value.

$$B = \log_2 N + P \log_2 P + (1-P) \log_2 \left[\frac{1-P}{N-1}\right] \tag{10}$$

$$\text{ITR} = B \times \frac{60}{t} \tag{11}$$

where N is number of stimulus, P is average performance, and t indicates time for each selection.[21]. Besides, a small number of stimuli in effective BCI systems indicates a low ITR value. However, in this study, all of the small number of stimulus data were shown to the participant in fixed order, and this signal was classified as a whole. In this way, repetitions for predicting a stimulus were avoided, and the classification time was reduced. In this study, since the classification time for a stimulus is low, the ITR value was obtained more successfully than similar systems. In our study, as seen in Table 2, the highest ITR value of 40.39 was obtained with the Bi-LSTM based on feature fusion method.

4. Discussion and conclusion

In this study, the EEG signals obtained with the Emotiv EPOC+ device for the BCI system using P300 signals were classified with Bi-LSTM network. Prior to classification, EEG signals were calculated by using instantaneous frequency change calculation and spectral entropy method. Designed 4 symbols were shown to the participants with a software developed in the Unity environment as stimulus. It was aimed to classify the EEG signals received from the participants for these 4 symbols. The classification carried on MATLAB was obtained from the EEG device, which contains 14 channels of which only O1 was utilized. In summary, the results obtained by the studies performed on the designed experimental mechanism show that Bi-LSTM networks achieved a high success rate of 98.6% in training data set, and 96.9% in test data set with its advanced structure.

Although it is difficult to compare the previous studies on this subject in the literature due to the use of different datasets and classification methods, some previously proposed studies were denoted in Table 3. When the average number of participants in previous studies is evaluated, it can be said that the number of 10 participants in our study is at a reasonable level. In addition, it was observed that there are a limited number of previous studies conducted with the Bi-LSTM method proposed in this study for the classification of P300 signals. As can be seen from the LSTM-based [15] study in Table 3, it is seen that the average accuracy value is 86.32%. Besides, when the average accuracy values in Table 3 are compared, it can be concluded that the average accuracy value of 96.9% obtained in this study is higher than the ones found in most of the previous

studies and is at an acceptable level. The feature extraction method and the high performance of the Bi-LSTM network presented in our study performed an important contribution to P300 signal analysis on EEG signals. When the ITR values in previous studies and the ITR values in this study are compared, it is seen that the ITR value of 40.39 is at a reasonable level.

Table 3. Comparison of previous studies proposed for classification of P300 signals.

Authors	**Year**	**Method**	**Datasets**	**Participant**	**Acc. %**	**ITR**	**Ref.**
HE et al.	2017	SVM	Their own dataset	8	92,7	-	[12]
KUNDU and ARI	2017	PCA and E-WSVMs	BCI Comp.	2	98	-	[40]
AYDIN et al.	2017	LDA	Their own dataset	10	93,27	30,9	[41]
VO, Kha, et al.	2018	EC, DT, and AL- SVM	Akimpech dataset	-	91,26	26,78	[42]
KSHIRSAGAR and LONDHE	2019	WE-DCNN	Their own dataset	10	92,64	55,45	[43]
JIN et al.	2019	WLDA	Their own dataset	116	80	51,3	[44]
ARICAN and POLAT	2019	PVBSC-ELDA	BCI Comp.	-	94,17	6	[45]
DITTHAPRON, et al.	2019	CNN-LSTM	BCI Comp.	-	86,32	-	[15]
RATCLIFFE and PUTHUSSERYPADY	2020	NNA	Their own dataset	10	91,3	12,2	[46]
LI et al.	2020	FLDA	Their own dataset	10	96	52	[47]
SANTAMARÍA-VÁZQUEZ, et al.	2020	CNN EEG inception	GIB-UVA ERP-BCI DATASET	73	84,6	25,64	[48]
ORALHAN, Zeki.	2020	3D CNN	BCI Comp.	-	94,22	6,64	[49]
SHUKLA et al.	2021	DCNN	Their own dataset	9	90,55	22,33	[50]
LIU et al.	2021	1D-CapsNet-64	BCI Comp.	-	96	7	[51]
ALVARADO-GONZÁLEZ et al.	2021	DeepConvNet	P300-LINI	22	90	-	[52]
LI et al.	2021	P-FLDA	Their own dataset	9	95,83	57,17	[53]
Our Method	2021	Bi-LSTM	Our Dataset	5	96,9	40,39	

Emotiv device is a device open to noise interference due to its structure. For this reason, good filtering and feature extraction is required when it is used in online brain computer interface systems. For this reason, in this study, instantaneous frequency components and power spectrum techniques of the signal are used as feature extraction method in classification via Bi-LSTM network. The performance of these feature extraction

techniques in online systems can be compared in future studies. In addition to these, it is planned to increase the performance by analysing the performance differences by using different feature extraction methods.

Participants in a wide age range were included in the study. Participants' hair density, head structure and inactivity performances emerge as a major factor at this point. The fact that the sensor pressure points of the device cannot be changed creates a big disadvantage at this point. Because of this disadvantage, sensor head points differ in individuals with different skull widths. For this reason, as the P300 signals are not very different among the individuals, the data of the 10 participants with the most reliable data were used. For future studies, it is planned to carry out the study online and to achieve the same performance in a shorter period of time. In addition, it is aimed to continue working with flex models of the device designed as a single piece used in this study in future studies. Moreover, in the study, icons with coloured components were preferred as the stimulus matrix. Analysis of the preferred method to investigate the superiority of coloured stimuli over black and white stimulus matrices can be evaluated in future studies. Finally, in future studies, it can also be provided to shorten the classification time of the focused character by developing experimental studies conducted on a single stimulus performed in this study.

Acknowledgement

This work was supported by Research Fund of the Sakarya University of Applied Sciences. Project Number: 2015-50-02-038. This work experimental protocol was approved 28.12.2016 dated and 16214662/050,01,04/2 numbered by Ethics Committee of the Sakarya University Faculty of Medicine.

Conflict of interest

The authors declare that there is no conflict of interest regarding the publication of this paper.

Data availability

The data used in this study can be provided by the author upon request.

References

[1] Wolpaw JR, Birbaumer N, McFarland DJ, Pfurtscheller G, Vaughan TM. Brain-computer interfaces for communication and control. Clinical Neurophysiology 2002; 113 (6): 767-791. doi: 10.1016/s1388-2457(02)00057-3

[2] Abdulkader SN, Atia A, Mostafa M-SM. Brain computer interfacing: Applications and challenges. Egyptian Informatics Journal 2015; 16 (2): 213-230. doi: 10.1016/j.eij.2015.06.002

[3] Sellers EW, Ryan DB, Hauser CK. Noninvasive brain-computer interface enables communication after brainstem stroke. Science Translational Medicine 2014; 6 (257): 7. doi: 10.1126/scitranslmed.3007801

[4] Beveridge R, Wilson S, Callaghan M, Coyle D. Neurogaming with motion-onset visual evoked potentials (mVEPs): adults versus teenagers. IEEE Transactions on Neural Systems and Rehabilitation Engineering 2019; 27 (4): 572-581. doi: 10.1109/tnsre.2019.2904260

[5] Wolpaw J, Wolpaw EW. Brain-Computer Interfaces: Something New Under The Sun. In: Wolpaw J, Wolpaw EW (editor). Brain-computer interfaces: principles and practice. Manhattan, NY, USA: Oxford University Press, 2012.

[6] Saevarsson S, Kristjánsson Á, Bach M, Heinrich SP. P300 in neglect. Clinical Neurophysiology 2012; 123 (3): 496-506. doi: 10.1016/j.clinph.2011.07.028

[7] Sambeth A, Maes JHR, Brankačk J. With long intervals, inter-stimulus interval is the critical determinant of the human P300 amplitude. Neuroscience Letters 2004; 359 (3): 143-146. doi: 10.1016/j.neulet.2004.01.064

[8] Farwell LA, Donchin E. Talking off the top of your head: toward a mental prosthesis utilizing event-related brain potentials. Electroencephalography and Clinical Neurophysiology 1988; 70 (6): 510-523. doi: 10.1016/0013-4694(88)90149-6

[9] Gu Z, Chen Z, Zhang J, Zhang X, Yu ZL. An online ınteractive paradigm for P300 brain–computer ınterface speller. IEEE Transactions on Neural Systems and Rehabilitation Engineering 2019; 27 (2): 152-161. doi: 10.1109/tnsre.2019.2892967

[10] Perez AF, Oliver MA, Salas G. Development of a brain-computer ınterface based on visual stimuli for the movement of a robot joints. IEEE Latin America Transactions 2016; 14 (2): 477-484. doi: 10.1109/tla.2016.7437182

[11] Iturrate I, Antelis JM, Kubler A, Minguez J. A noninvasive brain-actuated wheelchair based on a P300 neurophysiological protocol and automated navigation. IEEE Transactions on Robotics 2009; 25 (3): 614-627. doi: 10.1109/tro.2009.2020347

[12] He S, Zhang R, Wang Q, Chen Y, Yang T et al. A P300-based threshold-free brain switch and its application in wheelchair control. IEEE Transactions on Neural Systems and Rehabilitation Engineering 2017; 25 (6): 715-725. doi: 10.1109/tnsre.2016.2591012

[13] Wang M, Daly I, Allison BZ, Jin J, Zhang Y et al. A new hybrid BCI paradigm based on P300 and SSVEP. Journal of Neuroscience Methods 2015; 244: 16-25. doi: 10.1016/j.jneumeth.2014.06.003

[14] Kundu S, Ari S. A deep learning architecture for p300 detection with brain-computer ınterface application. IRBM 2020; 41 (1): 31-38. doi: 10.1016/j.irbm.2019.08.001

[15] Ditthapron A, Banluesombatkul N, Ketrat S, Chuangsuwanich E, Wilaiprasitporn T. universal joint feature extraction for P300 EEG classification using multi-task autoencoder. IEEE Access 2019; 7: 68415-68428. doi: 10.1109/access.2019.2919143

[16] Martínez-Cagigal V, Santamaría-Vázquez E, Gomez-Pilar J, Hornero R. Towards an accessible use of smartphone-based social networks through brain-computer interfaces. Expert Systems with Applications 2019; 120: 155-166. doi: 10.1016/j.eswa.2018.11.026

[17] Chen J, Wang H, Wang Q, Hua C. Exploring the fatigue affecting electroencephalography based functional brain networks during real driving in young males. Neuropsychologia 2019; 129: 200-211. doi: 10.1016/j.neuropsychologia.2019.04.004

[18] Oropesa E, Cycon HL, Jobert M. Sleep stage classification using wavelet transform and neural network. International computer science institute 1999.

[19] Van Hese P, Philips W, De Koninck J, Van de Walle R, Lemahieu I et al. Automatic detection of sleep stages using the EEG. In: 23rd Annual International Conference of the IEEE-Engineering-in-Medicine-and-Biology-Society; İstanbul, Turkey 2001. pp. 1944-1947.

[20] Kaur B, Singh D, Roy PP. Age and gender classification using brain-computer interface. Neural Computing & Applications 2019; 31 (10): 5887-5900. doi: 10.1007/s00521-018-3397-1

[21] Katyal EA, Singla R. EEG-based hybrid QWERTY mental speller with high information transfer rate. Medical & Biological Engineering & Computing 2021; 59 (3): 633-661. doi: 10.1007/s11517-020-02310-w

[22] Islam MK, Rastegarnia A, Nguyen AT, Yang Z. Artifact characterization and removal for in vivo neural recording. Journal of Neuroscience Methods. 2014; 226: 110-123. doi: 10.1016/j.jneumeth.2014.01.027

[23] Luke R, Wouters J. Kalman Filter Based Estimation of Auditory Steady State Response Parameters. IEEE Transactions on Neural Systems and Rehabilitation Engineering 2017; 25 (3): 196-204. doi: 10.1109/tnsre.2016.2551302

[24] Majumdar KK, Vardhan P. Automatic Seizure Detection in ECoG by Differential Operator and Windowed Variance. IEEE Transactions on Neural Systems and Rehabilitation Engineering 2011; 19 (4): 356-365. doi: 10.1109/tnsre.2011.2157525

[25] Martinez P, Bakardjian H, Cichocki A. Fully Online Multicommand Brain-Computer Interface with Visual Neurofeedback Using SSVEP Paradigm. Computational Intelligence and Neuroscience 2007; 2007: 094561. doi: 10.1155/2007/94561

[26] Dornhege G, Blankertz B, Curio G, Muller K-R. Boosting Bit Rates in Noninvasive EEG Single-Trial Classifications by Feature Combination and Multiclass Paradigms. IEEE Transactions on Biomedical Engineering 2004; 51 (6): 993-1002. doi: 10.1109/tbme.2004.827088

[27] Basiri M MA, Sk NM. Configurable Folded IIR Filter Design. IEEE Transactions on Circuits and Systems II: Express Briefs 2015; 62 (12): 1144-1148. doi: 10.1109/tcsii.2015.2468917

[28] Yang Z, Ren H. Feature Extraction and Simulation of EEG Signals During Exercise-Induced Fatigue. IEEE Access 2019; 7: 46389-46398. doi: 10.1109/access.2019.2909035

[29] Karimzadeh F, Boostani R, Seraj E, Sameni R. A Distributed Classification Procedure for Automatic Sleep Stage Scoring Based on Instantaneous Electroencephalogram Phase and Envelope Features. IEEE Transactions on Neural Systems and Rehabilitation Engineering 2018; 26 (2): 362-370. doi: 10.1109/tnsre.2017.2775058

[30] Zhao X, Zhang R, Mei Z, Chen C, Chen W. Identification of Epileptic Seizures by Characterizing Instantaneous Energy Behavior of EEG. IEEE Access 2019; 7: 70059-70076. doi: 10.1109/access.2019.2919158

[31] Wang H, Wu C, Li T, He Y, Chen P et al. Driving Fatigue Classification Based on Fusion Entropy Analysis Combining EOG and EEG. IEEE Access 2019; 7: 61975-61986. doi: 10.1109/access.2019.2915533

[32] Mesbah M, O' Toole JM, Colditz PB, Boashash B. Instantaneous frequency based newborn EEG seizure characterisation. EURASIP Journal on Advances in Signal Processing 2012; 2012 (1): 143. doi: 10.1186/1687-6180-2012-143

[33] Yildirim O, Baloglu UB, Tan R-S, Ciaccio EJ, Acharya UR. A new approach for arrhythmia classification using deep coded features and LSTM networks. Computer Methods and Programs in Biomedicine 2019; 176: 121-133. doi: 10.1016/j.cmpb.2019.05.004

[34] Zhao J, Mao X, Chen L. Speech emotion recognition using deep 1D & 2D CNN LSTM networks. Biomedical Signal Processing and Control 2019; 47: 312-323. doi: 10.1016/j.bspc.2018.08.035

[35] Hu X, Yuan S, Xu F, Leng Y, Yuan K et al. Scalp EEG classification using deep Bi-LSTM network for seizure detection. Computers in Biology and Medicine 2020; 124: 103919. doi: 10.1016/j.compbiomed.2020.103919

[36] Alkan A, Kiymik MK. Comparison of AR and Welch Methods in Epileptic Seizure Detection. Journal of Medical Systems 2006; 30 (6): 413-419. doi: 10.1007/s10916-005-9001-0

[37] Kaper M, Meinicke P, Grossekathoefer U, Lingner T, Ritter H. BCI Competition 2003—Data Set IIb: Support Vector Machines for the P300 Speller Paradigm. IEEE Transactions on Biomedical Engineering 2004; 51 (6): 1073-1076. doi: 10.1109/tbme.2004.826698

[38] Xu G, Ren T, Chen Y, Che W. A One-Dimensional CNN-LSTM Model for Epileptic Seizure Recognition Using EEG Signal Analysis. Frontiers in Neuroscience 2020; 14. doi: 10.3389/fnins.2020.578126

[39] Sindi H, Nour M, Rawa M, Öztürk Ş, Polat K. A novel hybrid deep learning approach including combination of 1D power signals and 2D signal images for power quality disturbance classification. Expert Systems with Applications 2021; 174: 114785. doi: 10.1016/j.eswa.2021.114785

[40] Kundu S, Ari S. P300 Detection with Brain–Computer Interface Application Using PCA and Ensemble of Weighted SVMs. IETE Journal of Research 2018; 64 (3): 406-414. doi: 10.1080/03772063.2017.1355271

[41] Aydin EA, Bay OF, Guler I. P300-Based Asynchronous Brain Computer Interface for Environmental Control System. IEEE Journal of Biomedical and Health Informatics 2018; 22 (3): 653-663. doi: 10.1109/jbhi.2017.2690801

[42] Vo K, Pham T, Nguyen DN, Kha HH, Dutkiewicz E. Subject-Independent ERP-Based Brain–Computer Interfaces. IEEE Transactions on Neural Systems and Rehabilitation Engineering 2018; 26 (4): 719-728. doi: 10.1109/tnsre.2018.2810332

[43] Kshirsagar GB, Londhe ND. Weighted Ensemble of Deep Convolution Neural Networks for Single-Trial Character Detection in Devanagari-Script-Based P300 Speller. IEEE Transactions on Cognitive and Developmental Systems 2020; 12 (3): 551-560. doi: 10.1109/tcds.2019.2942437

[44] Jin J, Li S, Daly I, Miao Y, Liu C et al. The Study of Generic Model Set for Reducing Calibration Time in P300-Based Brain–Computer Interface. IEEE Transactions on Neural Systems and Rehabilitation Engineering 2020; 28 (1): 3-12. doi: 10.1109/tnsre.2019.2956488

[45] Arican M, Polat K. Pairwise and variance based signal compression algorithm (PVBSC) in the P300 based speller systems using EEG signals. Computer Methods and Programs in Biomedicine 2019; 176: 149-157. doi: 10.1016/j.cmpb.2019.05.011

[46] Ratcliffe L, Puthusserypady S. Importance of Graphical User Interface in the design of P300 based Brain–Computer Interface systems. Computers in Biology and Medicine 2020; 117: 103599. doi: 10.1016/j.compbiomed.2019.103599

[47] Li M, Yang G, Xu G. The Effect of the Graphic Structures of Humanoid Robot on N200 and P300 Potentials. IEEE Transactions on Neural Systems and Rehabilitation Engineering 2020; 28 (9): 1944-1954. doi: 10.1109/tnsre.2020.3010250

[48] Santamaria-Vazquez E, Martinez-Cagigal V, Vaquerizo-Villar F, Hornero R. EEG-Inception: A Novel Deep Convolutional Neural Network for Assistive ERP-Based Brain-Computer Interfaces. IEEE Transactions on Neural Systems and Rehabilitation Engineering 2020; 28 (12): 2773-2782. doi: 10.1109/tnsre.2020.3048106

[49] Oralhan Z. 3D Input Convolutional Neural Networks for P300 Signal Detection. IEEE Access 2020; 8: 19521-19529. doi: 10.1109/access.2020.2968360

[50] Shukla PK, Chaurasiya RK, Verma S. Performance improvement of P300-based home appliances control classification using convolution neural network. Biomedical Signal Processing and Control 2021; 63: 16. doi: 10.1016/j.bspc.2020.102220

[51] Liu X, Xie Q, Lv J, Huang H, Wang W. P300 event-related potential detection using one-dimensional convolutional capsule networks. Expert Systems with Applications 2021; 174: 114701. doi: 10.1016/j.eswa.2021.114701

[52] Alvarado-González M, Fuentes-Pineda G, Cervantes-Ojeda J. A few filters are enough: Convolutional Neural Network for P300 Detection. Neurocomputing 2021; 425: 37-52. doi: 10.1016/j.neucom.2020.10.104

[53] Li M, Yang G, Liu Z, Gong M, Xu G et al. The Effect of SOA on An Asynchronous ERP and VEP-Based BCI. IEEE Access 2021; 9: 9972-9981. doi: 10.1109/access.2021.3050545